Third International Conference on Inverse Design Concepts and Optimization in Engineering Sciences (ICIDES-III), Editor: G.S. Dulikravich, Washington D.C., October 23-25, 1991.

OPTIMIZATION OF THE HEATING SURFACE SHAPE IN THE CONTACT MELTING PROBLEM

Sergei A. Fomin

Department of Appplied mathematics, Kazan State University, Kazan, 420008, USSR

and

Shangmo Cheng

Department of Power Engineering, Huazhong University of Science and Technology, Wuhan, 430074, China

ABSTRACT

The work is devoted to the theoretical analysis of contact melting by the migrating heat source with an arbitrary shaped isothermal heating surface.After the substantiated simplification the governing equations are transformed to the convenient for engineering calculations relationships. Analytical solutions are used for numerical prediction of optimal shape of the heating surface. Problem is investigeted for the constant and for temperature dependent physical properties of the melt.

1. INTRODUCTION

Melting of solids by contact with a heating surface takes place in numerous natural and technological processes. These processes are enumerated in the previous works [2, 4, 12–14, 22] devoted to contact melting problem and are divided into two groups. In one group the melting material lies on the heating surface and pressed against it by some external force (for instance, the force of the weight of the melting material). This situation arises when an unfixed solid melts in an enclosure [1, 16, 22] and in other contact melting devices used in industry [8]. Another group of applications involves a moving heat source melting its way through the surrounding solid. This situation arises in such fields as welding [21], geology [3], nuclear technology [9, 10] thermal drilling of rocks [4, 6, 18, 20] and glaciers [11, 17, 19]. Thermal drilling is commonly recognized now as the most effective method of boring glaciers. Boring rocks, sands and soil by thermopenetrators is a relatively new method in mining engineering. It has some advantages in comparison with traditional rotary drilling. The most considerable advantage of thermodrilling is that three major facts of excavation (rock fracturing, debris removal and wall stabilization) are accomplished in a single integrated operation.

This work is devoted to the theoretical analysis of the contact melting process by the moving heating source with an arbitrary shaped isothermal heating surface.

2. ANALYSIS

2.1. The physical model and governing equations.

Obviously every technological process where contact melting occurs has its own specific character. In particular case of thermodrilling, it is contact melting with a great specific load and heat energy, with arbitrary shaped heating surface. Thermopenetrators are radially symmetric and in some cases ring-shaped,

Third International Conference on Inverse Design Concepts and Optimization in Engineering Sciences (ICIDES-III). Editor: G.S. Dulikravich, Washington D.C., October 23-25, 1991.

or toroidal, with a large central hole for forming and extracting the core sample [6]. A schematic diagram of the contact melting for the thermodrilling conditions is shown in Fig.1. Axisymmetric heater −1 is penetrating into the melting solid −2 with the velocity V under the effect of applied external force F. The thermopenetrator is separated from the solid with a layer of melt −3, flowing along the thin channel between the heating surface $\sum_h$ and solid−liquid interface $\sum_m$. It is assumed that the solid−liquid interface is a sharply defined surface and melting occurs precisely at temperature t_m, melt flow is laminar and two−dimensional. Molten layer is assumed to be incompressible Newtonian liquid with a temperature dependent physical properties (except density). Experimental results [6, 15] indicated that the heat source velocity attains its quasi−steady, constant value V soon after initiation of melting. This fact justifies the next assumption of quasi−steady heat and mass transfer in the contact melting problem.

According to the physical model and assumptions enumerated above the governing differential equations of heat and mass transfer in the molten layer can be written as follows:

$$
\begin{aligned}
&\mathrm{div}\bar{v} = 0 \\
&\rho_L(\bar{v}\cdot\nabla)\bar{v} = \bar{G} - \rho_L \nabla p + \mathrm{div}T \\
&C_L\rho_L(\bar{v}\cdot\nabla t_L) = \mathrm{div}(\lambda_L \nabla t_L) + \Phi
\end{aligned} \tag{1}
$$

where T is the deviator part of the tensor of internal stresses; $\bar{v}$, p, t_L are the liquids velocity, pressure and temperature respectively; Φ represents the dissipative terms in heat transfer equation; C_L, ρ_L, λ_L liquid properties defined in Nomenclature; the rest of the symbols are standard.

It is convenient for further analysis to use two systems of coordinates fixed to the heating surface: cylindrical coordinates (r, z) and local orthogonal boundary layer coordinates S and ξ are indicated in Fig. 1.

Transforming (1) to non−dimensional form and using the similarity method in a preliminary analysis the main dimensionless parameters and numbers are generated [7]:

$$
Pe = \frac{Vd}{a_s},\ Ste = \frac{C_s(t_m - t_\infty)}{L},\ K_h = \left(\frac{\rho_s \mu_L^m V}{\rho_L W d}\right)^{1/3},\ K_c = \frac{C_s}{C_L^m},\ Re = V\rho_s d/\mu_L^m\ \ K_h,
$$

$$
Br = \frac{W\bar{P}_e}{C_L^m \rho_L (t_m - t_\infty)},\ \bar{P}e = \frac{PeK_\lambda K_h}{K_c},\ K_\lambda = \frac{\lambda_s}{\lambda_L^m},\ K_g = \rho_L gd/W \tag{2}
$$

All the quantities here are defined in the Nomenclature. Each of the dimensionless numbers (2) has an exact obvious physical meaning. In order to substantiate the simplification of the governing equations (1), the analysis of the values of these non−dimensional numbers for the concrete conditions of thermal drilling of ice and rock was carried out. Dimensionless parameter $K_h \sim 10^{-3} - 10^{-1}$ physically represents the ratio of characteristic thickness of the molten layer and characteristic size of the heating surface d; criterion $K_g \sim 10^{-3}$ is the ratio of the characteristic mass force of the melt and external force; Reynolds number $Re \sim 10^{-6} - 10^{-4}$; Brinkman number $Br \sim 10^{-5} - 10^{-4}$ represents the viscous dissipation of heat in the molten layer, Pecklet number $Pe \sim 10 - 100$; Stefan number $Ste \sim 1 - 10$; K_λ, $K_c \sim 1$.

After neglecting terms of $0(K_h, K_g, Re, Br)$ the governing nondimensional equations of heat and mass transfer in the molten layer will take the following form:

$$
\frac{1}{R^*}\frac{\partial}{\partial s}(R^* H u_s) + \frac{\partial u_\eta}{\partial \eta} = 0 \tag{3}
$$

$$
H^2\frac{dp}{ds} = \frac{\partial}{\partial \eta}\left(\mu\frac{\partial u_s}{\partial \eta}\right) \tag{4}
$$

Third International Conference on Inverse Design Concepts and Optimization in Engineering Sciences (ICIDES-III), Editor: G.S. Dulikravich, Washington D.C., October 23-25, 1991.

$$PcCH(Hu_s\frac{\partial\theta}{\partial s}+u_\eta\frac{\partial\theta}{\partial\eta})=\frac{\partial}{\partial\eta}(\lambda\frac{\partial\theta}{\partial\eta}) \tag{5}$$

where $\eta=\frac{\xi}{h}$, $P=p/w$, $S=s/d$, $H=h/K_h d$, $\mu=\mu_L/\mu_L^m$, $C=C_L/C_L^m$, $\lambda=\lambda_L/\lambda_L^m$, $R=r/d$, $u_s=\frac{v_s\rho_L}{V\rho_s}$, $u_\rho=\frac{v_\eta\rho_L}{V\rho_s}$, $\theta=\frac{t_L-t_m}{\bar{t}_h-t_m}$, $R=R(s)$–equation of generating line Γ_h of heating surface $\sum_h$; $h=h(s)$ –thickness of the molten layer mersured along the internal normal to Γ_h; v_s, v_η –longitude and transverse velocities in the molten layer; all the physical properties of liquid C_L, λ_L, μ_L are nondimensionalized by their values C_L^m,λ_L^m,μ_L^m at temperature t_m;reference temperature ($\bar{t}_h-t_m$) is determined after nondimensionalization of Stefans condition,

$$\bar{t}_h-t_m=\bar{P}cK_c(t_m-t_\infty) \tag{6}$$

Here t_∞ is initial temperature of melting material. In the equation (3) $\nu=0$ corresponds to the ring–shaped penetrator with a large central hole. In this case since the thickness of the liquid film is of $0(K_h)$ it is possible to ignore the axially symmetric behaviour of heat and mass transfer and to consider (r, z) as the Cartesian coordinates; $\nu=1$ corresponds to the continuous heating surface without hole.

The boundary conditions in dimensionless form are following

At the heating surface $\sum_h(\eta=0)$

$$u_s=u_\eta=0;\quad \theta=\theta_h; \tag{7}$$

$\theta_h=(t_h-t_m)/(\bar{t}_h-t_m)$; t_h is the unknown temperature on $\sum_h$

At the solid–liquid interface $\sum_m(\eta=1)$

$$u_s=0;\quad u_\eta=-\frac{dR}{ds};\quad \theta=0 \tag{8}$$

$$-\frac{1}{H}\frac{\partial\theta}{\partial\eta}|_{\eta=1}=[\frac{Q}{Pc}+(\frac{dR}{ds})/Ste];\ Q=(-\frac{\partial\theta_s}{\partial n})|_{\Sigma_m}; \tag{9}$$

where $\theta_s=(t_s-t_\infty/(t_m-t_\infty)$, t_s is a temperature of the solid material,n is an external relatively tomolten layer normal to $\sum_m$.

For the pressure in the exit points of the molten layer $s=s_1$ and $s=s_2$

$$P(s_1)=P(s_2)=0 \tag{10}$$

Since when $\nu=1$ it is only one exit point $s=s_2$ then in this case $s_1=0$ is the critical point where $u_s=0$ $dP/ds=0$.

The assumption of quasi–stationary heat and mass transfer couses the equality of external force F and the force of internal stresses in the molten layer. This condition with the defined accuracy of $0(K_h)$ in non–dimensional form is [4]

$$1=\frac{2}{R_2^2-R_1^2}\int_{R_1}^{R_2}RPdR \tag{11}$$

The function Q in Stefan condition (9) is the non–dimensional density of heat flux to the solid from surface $\sum_m$ It's value depends on the temperature distribution in the solid and is obtained from the solution of the heat transfer problem which is the same as the problem of temperature distribution in the surrounding weldpool material [21]:

Third International Conference on Inverse Design Concepts and Optimization in Engineering Sciences
(ICIDES-III), Editor: G.S. Dulikravich, Washington D.C., October 23-25, 1991.

$$-\mathrm{Pe}\frac{\partial\theta_s}{\partial Z}+\frac{\partial^2\theta_s}{\partial Z^2}+\frac{1}{R^\nu}\frac{\partial}{\partial R}(R^\nu\frac{\partial\theta_s}{\partial R})=0;\quad \nu=0,1; \tag{12}$$

$$\theta_s|_{\Sigma_m}=1;\quad \lim_{R^2+Z^2\to\infty}\theta_s=0;\quad \theta_s|_{\Sigma_f}=\theta_f;\quad (R,Z)=(r,z)/d; \tag{13}$$

θ_f– is temperature distribution on surface $\sum_f$, formed after melting (Fig.1). Problem (12) (13) was solved in [4, 18] numerically by the boundary element method.

2.2. Analytical solutions

In [4] it was proved that boundary value problem (12), (13) admits an analytical solution as a function of one independent variable when and only when the generating curve $\Gamma_m$of $\sum_m$ is parabola. In parabolic coordinates σ and τ related to the coordinates R and Z by $R=\tau\sigma$, $Z=0.5(\sigma^2-\tau^2)$ with boundary conditions on $\sum_m$; $\tau=\tau_m$,$\theta_s=1$, in infinity: $\tau\to\infty$, $\theta_s\to 0$, equasion (12) has the following solution

$$\theta_s=\begin{cases}\mathrm{Ei}(-\frac{\mathrm{Pe}}{2}\tau^2)/\mathrm{Ei}(\frac{-\mathrm{Pe}}{2}\tau_m^2), & \nu=1\\ \mathrm{erfc}(\sqrt{\frac{\mathrm{Pe}}{2}}\tau)/\mathrm{erfc}(\sqrt{\frac{\mathrm{Pe}}{2}}\tau_m), & \nu=0\end{cases} \tag{14}$$

where $\mathrm{erfc}(x)=\frac{2}{\sqrt{\pi}}\int_x^\infty \exp(-u^2)du$, $\mathrm{Ei}(-x)=\int_1^\infty\frac{\exp(-xu)}{u}du \quad x>0$

According the formulae (9) and (14) the heat flux distribufion on $\sum_m$ is

$$Q=\frac{\mathrm{Pe}\ e^{-\alpha^2}\tau_m}{\sqrt{\tau_m^2+\sigma^2}}\Big/\begin{cases}\alpha^2\mathrm{Ei}(-\alpha^2), & \nu=1\\ \sqrt{\pi}\,\alpha\mathrm{erfc}(\alpha), & \nu=0\end{cases} \tag{15}$$

where $\alpha^2=\mathrm{Pe}\tau_m/2$ Taking into account the fact that the distance between $\sum_h$ and $\sum_m$ is the value of $0(K_h)$ we can rewrite (15) with the accuracy of $0(K_h)$

$$Q=\mathrm{Pe}\cdot e^{-\alpha^2}\frac{dR}{ds}\Big/\begin{cases}\alpha^2\mathrm{Ei}(-\alpha^2), & \nu=1\\ \sqrt{\sigma}\,\alpha\mathrm{erfc}(\alpha), & \nu=0\end{cases} \tag{16}$$

After simple transformation of equations (3) and (4) with invoked boundary conditions (7), (8) and (10) the velocities and pressure distribution in the molten Layer are obtained

$$u_s=\frac{R^{\nu+1}-R_*^{\nu+1}}{(\nu+1)HDR^\nu}\int_0^\eta\frac{\eta_0-\eta}{\mu}d\eta \tag{17}$$

$$u_\eta=-\frac{1}{(\nu+1)R^\nu}\frac{\partial}{\partial s}\left[\frac{(R^{\nu+1}-R_*^{\nu+1})}{D}\varphi\right] \tag{18}$$

$$P=\frac{1}{\nu+1}\int_s^{s_2}\frac{R^{\nu+1}-R_*^{\nu+1}}{R^\nu H^3 D}ds \tag{19}$$

where $D=\int_0^1\frac{(\eta-\eta_0)}{\mu}\eta d\eta$, $\eta_0=\int_0^1\frac{\eta d\eta}{\mu}\Big/\int_0^1\frac{d\eta}{\mu}$

$$\varphi=\eta\int_0^\eta\frac{\eta_0-\eta}{\mu}d\eta-\int_0^\eta\frac{\eta_0-\eta}{\mu}\eta d\eta$$

R_* is a critical point which is determined by (19) and the boundary coudition $P(s_1)=0$

Third International Conference on Inverse Design Concepts and Optimization in Engineering Sciences (ICIDES-III), Editor: G.S. Dulikravich, Washington D.C., October 23-25, 1991.

$$R_{*}^{\nu+1} = \int_{s_1}^{s_2} \frac{R ds}{H^3 D} \Big/ \int_{s_1}^{s_2} \frac{ds}{R^{\nu} H^3 D} \tag{20}$$

when $\nu = 1$ it is supposed that $R_* = 0$

According the assumption $\theta_h = \text{const}$ the temperature distribution in the molten layer is sought as a function of one independent variable η

$$\theta = \theta(\eta) \tag{21}$$

As follows from interfacial condition (9) in this case

$$H\frac{dR}{ds} = \overline{H} = \text{const.} \tag{22}$$

Last formulae (22) and (21) simplify equalities (18), (19)

$$u_{\eta} = -\frac{1}{D}\frac{dR}{ds}\varphi(\eta) \tag{23}$$

$$P = \frac{1}{(\nu+1)D}\int_{s}^{s_2} \frac{R^{\nu+1} - R_{*}^{\nu+1}}{H^3 R^{\nu}} ds \tag{24}$$

and heat transfer equation in the molten layer

$$-\frac{\overline{\text{Pc}H}\varphi(\eta)}{D}\frac{d\theta}{d\eta} = \frac{d}{d\eta}(\lambda\frac{d\theta}{d\eta}) \tag{25}$$

Integration of this equation with the associated boundary conditions

$$\theta|_{\eta=1} = 0; \quad -\frac{d\theta}{d\eta}|_{\eta=1} = \overline{H}E; \quad E = \frac{Q}{Pe\frac{dR}{ds}} + \frac{1}{Ste} \tag{26}$$

reduce to the following relationship

$$\theta(\eta) = E\overline{H}\int_{\eta}^{1}\frac{1}{\lambda}\exp(\frac{\overline{PcH}}{D}\int_{\eta}^{1}\frac{\varphi C}{\lambda}d\eta)d\eta \tag{27}$$

puting in (27) $\eta = 0$ the temperature of the heating surface is determined

$$\theta_h = E\overline{H}\int_{0}^{1}\frac{1}{\lambda}\exp(\frac{\overline{PcH}}{D}\int_{\eta}^{1}\frac{\varphi C}{\lambda}d\eta)d\eta \tag{28}$$

In order to simplify further computations assume that Γ_h is specified by the equation $Z = A(R - R_*)^2$. In this case heat flux distribution Q is determined by the equality (16), where

$$\frac{dR}{ds} = \frac{1}{\sqrt{1 + 4A^2(R - R_*)^2}}$$

P(s) introduction into (11) yields

$$\overline{H}^3 = \frac{1}{(R_2^2 - R_1^2)(\nu+1)^2 D}\int_{R_1}^{R_2}\frac{R(R^{\nu+1} - R_{*}^{\nu+1})}{1 + 4A^2(R - R_*)^2}dR \tag{29}$$

where $R_1 = R_* = 0$ if $\nu = 1$

One of the most important characteristics of contact melting is the heat energy removal from the heating surface to the melt. Combining heat energy definition in non-dimensional form

$$N = 2\pi\int_{R_1}^{R_2}\frac{R}{\overline{\overline{H}}}(-\lambda\frac{d\theta}{d\eta})|_{\eta=0}dR$$

with the equation (27) we have

Third International Conference on Inverse Design Concepts and Optimization in Engineering Sciences
(ICIDES-III), Editor: G.S. Dulikravich, Washington D.C., October 23-25, 1991.

$$N = \pi(R_2^2 - R_1^2)E\exp(\frac{\overline{Pe}\overline{H}}{D}\int_0^1 \frac{c\varphi}{\lambda} d\eta) \tag{30}$$

The quantity of heat energy calculated according (30) excesses the minimum heat power N_0 which is necessary to sustain the chosen melting velocity V. In non–dimensional form

$$N_0 = \pi(R_2^2 - R_1^2)(1 + 1 / Ste)$$

Here N_0 in comparison with N does not contain the energy rate for heating melt and useless heat dissipation in the surrounding thermopenetrator solid material.

The main scope of present paper is to elucidate the influence of the heating surface shape upon the effectivety of the contact melting process. Defining efficiency of the heating surface as a ratio $\beta = N_0 / N$ we'll have

$$\beta = \frac{1 + \frac{1}{Ste}}{E}\exp(-\overline{Pe}\overline{H} / D \quad \int_0^1 \frac{c\varphi}{\lambda} d\eta) \tag{31}$$

Equations (23), (24), (27)–(31) simulate heat and mass transfer processes in contact melting problem with the accuracy of $0(K_h)$. They are convenient for prediction of contact melting process for materials with variable physical properties such as different kinds of rocks and sands.

When the physical properties of melt are constant (for example in the case of ice melting) equations (17), (23), (24), (27), (28), (30), (31). allows the considerable simplification.

$$u_s = \frac{6(R^{\nu+1} - R_*^{\nu+1})}{(\nu + 1)R^\nu H}\eta(1 - \eta) \tag{32}$$

$$u_\eta = -\frac{dR}{ds}\eta^2(3 - 2\eta) \tag{33}$$

$$P = \frac{12}{\nu + 1}\int_s^{s_2} \frac{R^{\nu+1} - R_*^{\nu+1}}{H^3 R^\nu} ds \tag{34}$$

$$\theta = E\overline{H}\exp(\overline{Pe}\overline{H} / 2 \quad \int_\eta^1 \exp[\overline{Pe}\overline{H}\eta^3(1 - 0.5\eta)]d\eta \tag{35}$$

$$N = \pi(R_2^2 - R_1^2)E\exp(\frac{\overline{Pe}\overline{H}}{2}) \tag{36}$$

$$\beta = \frac{(1 + \frac{1}{Ste})}{E}\exp(-\frac{\overline{Pe}\overline{H}}{2}) \tag{37}$$

3. RESULTS

Numerical prediction of u_s, u_η, P, H, θ, β and other quantities of interest is carried out for ice and rock thermodrilling conditions. All the calculations of rock melting are based on equations (23), (24), (27) —(31). Relatively complete description of basalt physical properties at high temperature is available in [5, 6]. Non–linear equation (27) is solved numerically by the iteration procedure. After this other quantities are obtained automatically in a view of equations (23), (24), (28)—(31). As the initial estimate of iterative process solution (35) is chosen. When the ice boring process is investigated formulae (29), (32)—(37) are used. The values of ice physical properties one can find for example in [4, 17, 19]. Effectiveness of the heating surface is estimated by the value of parameter β. It is shown in previous works [4, 17] that in com-

Third International Conference on Inverse Design Concepts and Optimization in Engineering Sciences
(ICIDES-III), Editor: G.S. Dulikravich, Washington D.C., October 23-25, 1991.

parison with the other (cone–shaped, sphere–shaped, etc.) thermopenetrators of the same power output the parabolic shaped penetrator attains the highest melting velocity, Therefore present paper is devoted to more detail analysis of contact melting with parabolic heating surface. The elongation of the surface is characterized by the value of shape parameter A. The results of numerically predicted efficiency as a function of A for different conditions of ice and rock melting are plotted in Fig. 2. Numerical results indicates that for slow melting when heat transfer in the molten layer is of minor significance and in the contrary the heat dissipation increases the flat heating surface ($A < 1$) is more effecfive. Vice versa for high speed melting the heat energy rate in the melt is dominating in comparison with the dissipation in surrounding solid material. So in this case the elongate form of heating surface is preferable. According the calculations presented in Fig.2 there is the interval for melting velocities when the definition of the optimal shape is not trivial. For toroidal penetrator ($\nu = 0$)and ice melting conditions $20 < Pe < 55$; for non–coring penetrator ($\nu = 1$) and rock melting conditions $40 < Pe < 75$. In order to find the maximum of β and the corresponding value of A, the derivative of β with respect to A is calculated. When the problem is non–linear and the physical properties of the melt depend on temperature the derivative is calculated numerically; when μ, c, λ are constants it is feasible to calculate β'_A analytically. In a view of relationship (37) the equation $\beta'_A = 0$ for computation of the optimal A can be written as follows: $-\bar{P}e\bar{H}'_A E - E'_A = 0$.

This simple equation is solved by dividing segment in half method.

NOMENCLATURE

A – shape parameter of the heating surface;
a – thermal diffusivity;
c – specific heat;
d – characteristic size of heating device;
F – external force;
G – mass force;
g – acceleration;
h – melt layer thickness;
L – latent melting heat;
P – pressure;
Q – heat flux density;
r, z – cylindrical coordinates defined in Fig.1;
r_1– internal radius of the heating device;
r_2– external radius of the heating surface;
s_1, s_2– coordinates of the end points of generating curve of the heating surface;
t – temperature; $\bar{v}$–velocity of the molten layer;
v_s, v_η– longitude and transverse velocities in the molten layer;
V – melting velocity;
s,ξ– longitudinal and transverse local coordinates in the molten layer defined in Fig. 1;
W–specific axial load from heating device side ($W = \dfrac{F}{\pi(r_2^2 - r_1^2)}$)
β– efficiency;
Γ– generating curve of surface $\sum$;
λ– thermal conductivity;
μ–dynamic viscosity coefficient;
ρ– density;
σ, τ– parabolic coordinates.

Third International Conference on Inverse Design Concepts and Optimization in Engineering Sciences
(ICIDES-III), Editor: G.S. Dulikravich, Washington D.C., October 23-25, 1991.

Indices:

L – liquid phase;
s – solid phase;
* – critical point;
h – heating surface;
m – melting surface;
∞ – value in infinite point.

All the non–dimensional parameters, numbers and functions are determined in the text: (2), (5), etc.

REFERENCES

[1] Barcis, M. and Beer, H. (1984). "An analytical solution of the heat transfer process during melting of unfixed solid phase change material inside a horizontal tube", Int. J. Heat Mass Trasfer, v.27, pp.739–746.

[2] Bejan, A. and Litsek, P. A. (1989), "The contact heating and lubricating flow of a body of glass", Int. J. Heat Mass Transfer, v.32, No4, pp.751–760.

[3] Birth, F. S. (1975), "Conduction heat flow anomalies over a hot spot in moving medium", J. of Geophysical Research, v.80, pp.4825–4827

[4] Chistyakov, V. K., Fomin, S.A. and Chugunov, V.A. (1984), "Heat mass Tansfer in contact melting", Kazan State Univ. Press, Kazan (in Russian).

[5] Filatoff, N., Lasek, A, (1989), "On variable viscosity magma flow", Int. J. Heat Mass Transfer, v.32, No. 12, pp.2485–2495.

[6] Fisher, N. (1976), "Thermal analysis of some subterrene penetrators", J. Heat Transfer, v.98, No. 3, pp.485–490.

[7] Fomin, S. A. (1988), "Mathematical modeling of heat and mass transfer in contact melting", Issled po priklad. Matem, v.16 pp.105–122 (in Russian).

[8] Griffin, O. M. (1970), "On the melting solid to non–Newtonian fluids", Chem. Eng. Science, v. 25, No.1, pp.109–117.

[9] Jansen, G. and Stepnewski, D. D. (1973), "Fast reactor fuel interactions with floer material after a hypothetical core meltdown", Nuclear technology, v. 17, pp.85–96.

[10] Logan, S. E. (1974), "Deep self–burial of radiative waste by rock melting capcules", Nuclear Technology. v.21 pp.111–124.

[11] Mellor, M. and Sellman, P. V. (1974), "General considerations for drill system design, Ice–core drilling", Proc. of Symp. Univ. of Nebraska, Lincoln, 28–30 August, pp. 77–111.

[12] Moallemi, M. K. and Viskanta, R. A. (1986), "Analysis of close contact melting heat transfer", Int. J. Heat Mass Transfer, v.29, No.6, pp.855–867.

[13] Moallemi, M. K. and Viskanta, R.A. (1986), "Analysis of melting around a moving heat source", Int. J. Heat Mass Transfer, v.29, No.8, pp.1271–1282.

[14] Moallemi, M. k. and Viskanta, R. A. (1985), "Melting around a migrating heat source", J. Heat Transfer, v.107, No.2, 451–458.

[15] Moallemi, M. K. and Viskanta, R. (1985), "Experiments of fluid flow induced by melting around a migrating heat source", J. Fluid Mech; v.157, pp.35–51.

[16] Moore, F.E and Bayzitoglu, Y. (1982), "Melting within a spherical enclosure", J. Heat Transfer, v.104, pp.19–23.

[17] Pudovcin, M. A., Salamatin, A. N., Fomin, S. A, and Chistyakov, V. K. (1988), "Effect of a thermal drill on hot–point ice boring performance", Journal of Soviet Mathematics, v.43, No. 3, pp.2496–2505.

[18] Salamatin, A. N., Fomin, S. A., Chistyakov, V. K. and Chugunov, V. A. (1984), "A mathematical description and calculation of contact melting", J. of Engineering Physics, v.XLVII, No. 3, pp.439–446.

[19] Shreve, R. L. (1962), "Theory of performance of isothermal solidnose hot points boring in temperate ice", J. of Glaciology, v.4, No.32, pp.151–160.

[20] The subterrene program. Mini–review 75–2 (1975), Los Alamos scientific laboratory, Los Alamos, New Mexico, USA.

[21] Thompson, M. E. and Szekely, J. (1989), "The transient behavior of weldpools with the deformed free surface", Int. J. Heat Mass Transfer, v.32, NO.6, pp.1007–1019.

[22] Webb, B. W., Moallemi, M. K and Viskanta, R. A. (1987), "Experiments of meltig unfixed ice in a horizontal cylindrical capsule". J. Heat Transfer, v.109, pp.454–459.

Third International Conference on Inverse Design Concepts and Optimization in Engineering Sciences (ICIDES-III), Editor: G.S. Dulikravich, Washington D.C., October 23-25, 1991.

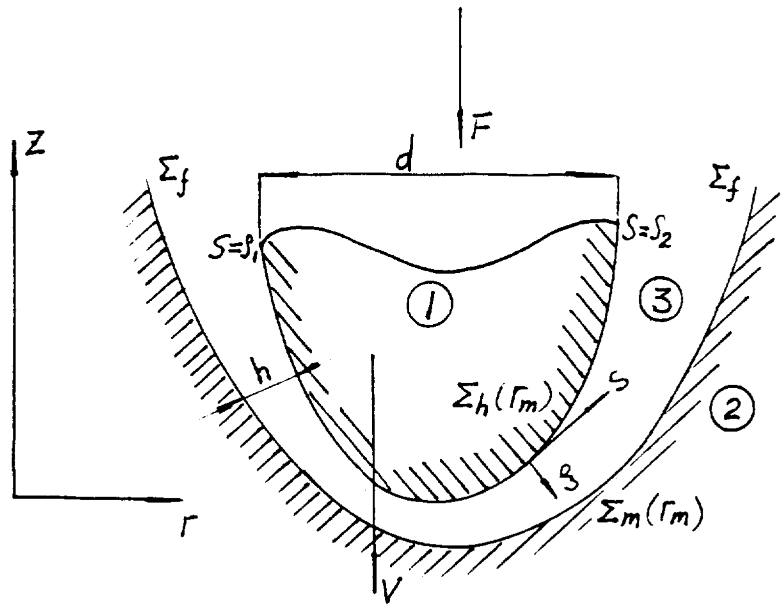

Fig. 1. Schematic representation of the contact melting process: 1–heating device, 2–melting solid, 3–molten layer.

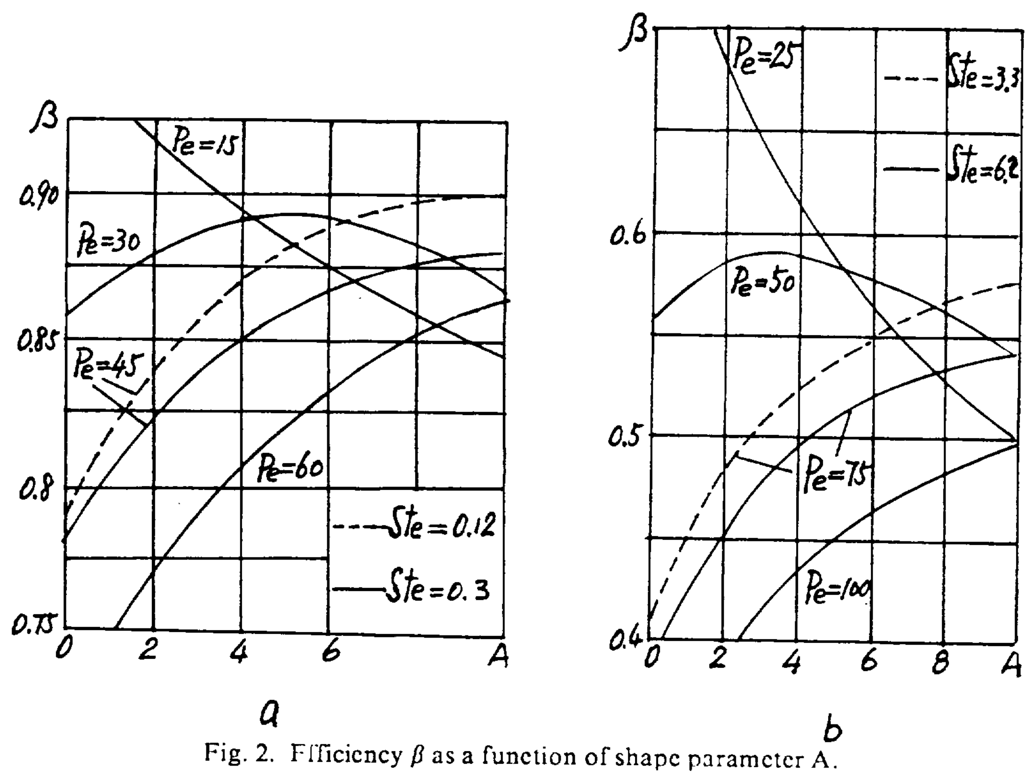

Fig. 2. Efficiency β as a function of shape parameter A.

a) Ice boring conditions; $\nu=0$, $R_* = 3.2$ (ring shaped penetrator)

b) Rock boring conditions; $\nu=1$, $R_* = R_1 = 0$ (non–coring penetrator)